Hydrogen Splittings of Bis-Bicyclic Hydrazine Radical Cations

Stephen F. Nelsen,*,† Peter A. Petillo,† James De Felippis,† Yichun Wang,† Ling-Jen Chen,† Maria J. R. Yunta,† and Franz A. Neugebauer‡

Contribution from the S. M. McElvain Laboratories of Organic Chemistry, Department of Chemistry, University of Wisconsin, 1101 West University Avenue, Madison, Wisconsin 53706-1380, and Abteilung Organische Chemie, Max-Plank-Institut für medizinische Forschung, 6900 Heidelberg 1, FRG

Received January 11, 1993

Abstract: ^{1}H-NMR spectra of bis-bicyclic hydrazine radical cations allowed determination of the magnitude and sign of the proton splitting constants under ~2 G, and assignments to position using deuterium labeling were made for several cases. ENDOR spectra measured the hydrogen splittings over 2 G. Bridgehead hydrogen splitting constants for sesquibicyclic compounds (bis-*N*,*N*'-bicyclics) were observed in the range –0.10 to +0.14 for six examples containing 2,3-diazabicyclo[2.2.2]octyl rings, –0.14 to –0.04 for two 2,3-diazabicyclo[2.2.2]octenyl compounds, +0.02 to +0.21 for four compounds containing 5,6-diazabicyclo[3.2.2]nonyl and -nonenyl rings, and +0.35 to +0.84 for compounds containing 2,3-diazabicyclo[2.2.1]heptyl rings. There is not a simple correlation of these bridgehead splitting constants with the lone pair N, C–H_b dihedral angle. For the nine sesquibicyclic hydrazine radical cations studied, the *exo* splittings in dimethylene bridges were positive, and the *endo* splittings were negative in sign. Examination of the W and non-W *exo* γ hydrogen splittings in systems containing bicyclo[2.2.2]octyl rings allowed estimation of the energy difference between double nitrogen inversion conformations.

Introduction

It has been known since the middle 1960s that ^{1}H-NMR could be used to measure both the sign and magnitude of relatively small hyperfine splitting constants, a(H), for radicals,[1] but experimental difficulties plagued the accuracy of the numbers obtained. The electron nuclear coupling manifests itself in the NMR as a contact chemical shift of the observed nuclei in the paramagnetic species as compared to those of a diamagnetic precursor, a $\Delta\delta$ value. As pointed out by Hausser and co-workers,[2] the relationship between $\Delta\delta_X$ for a paramagnetic nucleus X in a radical is given by eq 1, which for hydrogens at the 300 K

$$\Delta\delta_X = -a(X)\gamma_e{}^2h/8\pi\gamma_X kT \text{ gauss/gauss} \quad (1)$$

temperature used in this work corresponds to the relationship given in eq 2. An upfield shift of the paramagnetic species occurs

$$\Delta\delta_H(300\text{ K})/-a(H) = 73.76 \text{ ppm/gauss} \quad (2)$$

when a(H) is negative, and a downfield shift occurs when a(H) is positive. These equations, however, do not account for changes in bulk sample magnetic susceptibility as a function of paramagnetic sample concentration, and these effects, combined with use of internal instead of external referencing, are large enough to have caused incorrect and widely varying reports of a(H) measured by NMR for di-*tert*-butyl nitroxide (**1**).[3] The use of FT-NMR techniques to signal average and properly reference the spectra, and inclusion of concentration dependencies give rise

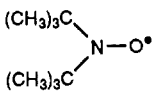

1

to a(H) values which agree with ESR and ENDOR measurements.[3] Line widths increase approximately as $(\Delta\delta)^2$, causing both overlap of signals and low signal-to-noise when a(H) is above a few tenths of a gauss. High total radical concentration narrows the lines, and it was discovered early that the relatively unreactive **1** is a useful solvent for NMR studies of radicals.[1]

In this work we report the application of ^{1}H- and ^{2}H-NMR to the measurement and assignment of splittings for the radical cations of several bis-bicyclic hydrazine derivatives and related compounds. Our NMR studies were all carried out in CD_3CN at 300 K. The commercially available and relatively difficult to oxidize **1** can usually be employed as a dopant for hydrazine radical cations with formal potentials for oxidation E^f up to about +0.1 V vs SCE. Doping allows extrapolation of the observed δ(paramagnetic) values to zero radical concentration and narrows the lines sufficiently to resolve closely spaced resonances and permit detection of larger $\Delta\delta$ peaks. Total radical concentrations on the order of 1 M prove necessary to observe lines when a(H) approaches 2 G, and we have not been able to observe signals for larger a(H) hydrogens by NMR. We have not found a successful dopant for more difficultly oxidized species.

Results

Comparison of Information Available from NMR and ENDOR. We studied radical cations $\mathbf{2}^{\bullet+}$–$\mathbf{5}^{\bullet+}$ to establish the utility of NMR for determination of ESR splitting constants of these compounds, and comparisons of the numbers obtained with previously

† University of Wisconsin.
‡ Max-Plank-Institut für medizinische Forschung.

(1) For reviews on NMR of paramagnetic species, see: (a) Orrell, K. G. NMR of Paramagnetic Species. In *Nuclear Magnetic Resonance (Specialists Periodical Reports)*; Webb, G. A., Ed.; The Royal Society of Chemistry: London, 1989; Vol. 18, pp 369, 376. (b) *N.M.R. of Paramagnetic Molecules: Principles and Applications*; Le Mar, G. N., Horrocks, W., Jr., Holm, J. R., Eds.; Academic Press: New York, 1973. (c) de Boer, E.; van Willigen, H. *Prog. Nucl. Magn. Reson. Spectrosc.* **1967**, 111. (d) Eaton, D. R.; Phillips, W. D. *Advances in Magnetic Resonance*; Academic Press: New York, 1965; p 103.

(2) Hausser, K. H.; Brunner, H.; Jochims, J. C. *Mol. Phys.* **1965**, *10*, 253.

(3) Petillo, P. A.; De Felippis, J.; Nelsen, S. F. *J. Org. Chem.* **1991**, *56*, 6496.

0002-7863/93/1515-5608$04.00/0

Table I. Summary of NMR and ESR/ENDOR Data for $2^{\bullet+}$–$5^{\bullet+}$

species	hydrogen, type	δ(n),[a] ppm	δ(c)^0,[a] ppm	a(H)$_{NMR}$, G	a(H)$_{ESR/END}$, G
$2^{\bullet+}$	1, b	3.18[b]	+74.7	+0.97	0.99 (4H)[c]
	2e, γe	1.45	+95.1	+1.27	1.28 (8H)
	2a, γa	2.06	−38.2	−0.55	0.59 (8H)
	3e, δe	1.55	+115.1	+1.54	1.60 (4H)
	3a, δa	1.93	+22.9	+0.28	0.27 (4H)
$3^{\bullet+}$	1, b	3.83	+39.5	+0.48	
	2e, γe	1.41	+57.0	+0.76	
	2a, γa	2.03	−24.4	−0.36	
	3e, δe	1.50	+77.4	+1.03	
	3a, δa	1.95	+13.9	+0.16	
	arom	6.85	−131.7	−1.88	
$4^{\bullet+}$	1, b	3.39	unobs		4.49 (4H)[d]
	2e, γe	1.25	+80.9	+1.08	1.03 (4H)
	2a, γa	1.80	−19.4	−0.28	0.24 (4H)[e]
	3e, δe	1.35	unobs		3.43 (2H)
	3a, δa	1.48	+47.3	+0.62	unobs
	6x, γx	1.95	−70.9	−0.98	unobs
	6n, γn	1.98	−11.1	−0.17	unobs
$5^{\bullet+}$	exo, x	~2.1[f]	unobs		+2.06 (8H)[f]
	endo, n	~2.1	−29.6[g]	−0.43	−0.31 (8H)
	brid, b	4.26	+11.6[g]	+0.10	+0.06 (4H)

[a] δ(n) and δ(c) in Tables I–III refer to neutral and radical cation chemical shifts, respectively. λ(c)^0 was measured at 300 K, from spectra taken with varying amounts of DBNO as spin relaxant, extrapolated to zero total radical concentration. [b] From reference 4. [c] From reference 5; at 243 K in CH_2Cl_2. The number of hydrogens was determined by ESR simulation; the signs of the splitting constants were not determined. [d] From reference 6; at 240 K in CH_2Cl_2. The sign of a(H) was not determined. [e] Position not assigned. [f] Reference 7; in 19:1 CH_2Cl_2/CF_3CO_2H at 240 K. [g] At 93 mM in CD_3CN, not extrapolated to zero radical concentration (see text).

published ESR and ENDOR data[4-7] appear in Table I. Excellent agreement between the methods was found for $2^{\bullet+}$, where both

2 3

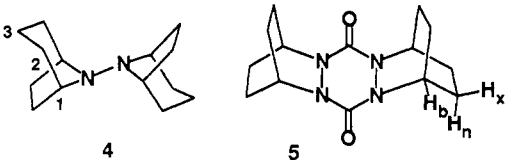

4 5

methods allowed the measurement of all five splitting constants. ENDOR results are not available for comparison with the NMR result for $3^{\bullet+}$, but there is excellent correspondence of splittings for $2^{\bullet+}$ and $3^{\bullet+}$, as expected from their structural similarity. The results for $4^{\bullet+}$ illustrate the differences between NMR and ENDOR as methods for measuring splitting constants. NMR could not measure the two large (a(H) > 2 G) splittings; but all five small splittings present were detected, and the splitting constant sign was unambiguously determined. The ENDOR was especially noisy for this species, and only two of the small splittings were detected; the positive W plan γ_{eq} splitting was not resolved from the negative non-W γ_{ax} splitting, and the three smallest splittings were lumped together. Labeling studies which would prove the positional assignments have not been carried out, but knowledge of the sign of a(H) makes assignments more certain. The results for $5^{\bullet+}$ demonstrate a definite limitation of the NMR method. E^f for formation of $5^{\bullet+}$ is 0.78,[7] far too high to allow use of **1** as a dopant, and only a single 0.093 M concentration was studied. The signal corresponding to the +2.03 G *exo* splitting could not be observed (it probably would have been if total radical concentration could have been increased an order of magnitude), and the a(H) values obtained show poorer agreement with the ENDOR values than for cases in which δ(cat) values could be properly extrapolated to zero radical concentration.

The bulk of this work concerns sesquibicyclic hydrazine radical cations, where the large number of small splittings typically present leads to little resolution for ESR spectra and, as shown by data reported here, even ENDOR has substantial difficulties. Nine sesquibicyclic species (**6–14**) whose structures are shown below

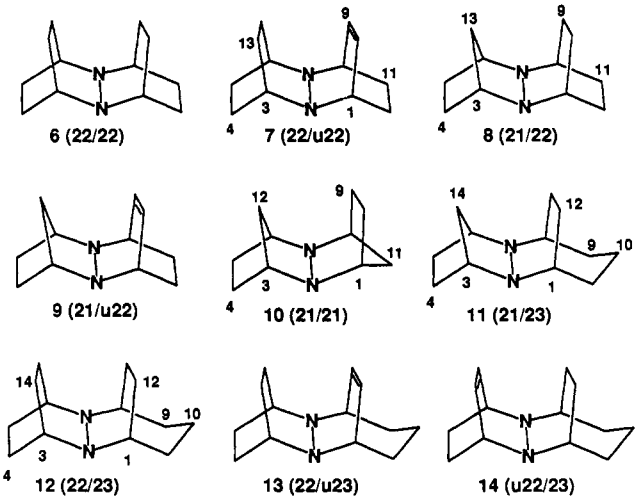

were studied. To prevent having to continually check drawings to identify the compounds, designations giving the sizes of the two bicyclic systems fused at the nitrogens will be used where convenient. The nitrogen-containing bridges have two atoms by definition; the sizes of the other two bridges are listed. Only the diastereomer shown is present for **9**, **11**, **13**, and **14**, and the double N inversion form (which we shall refer to as invertomer for convenience) of the radical cation assigned as the more stable one is that illustrated.

Neutral Sesquibicyclic Hydrazine NMR Chemical Shifts. The spectra of sesquibicyclic hydrazines are complex and show some overlapping hydrogens even at 500 MHz, and proper assignments have not been published. One hydrogen of the one-carbon bridge of **21/u22** appears as a rather narrow doublet (^2J 10.0 Hz) at 0.65 δ, which moves to 1.27 δ upon hydrogenation to **21/22**. We earlier[8] misassigned this hydrogen as *syn* on the basis of an incorrect double-bond shielding-cone argument and repeated this misassignment for similar compounds. The diastereomer is that shown (proven by an X-ray structure to be published elsewhere), but the upfield hydrogen is the *anti* one, which is in W plan with the nitrogen lone pairs. The *syn* hydrogen appears as a doublet of apparent quintets (J ~ 2.4 Hz) because of similar sized bridgehead and W plan couplings. Assignments of the ^{1}H spectra appear in the Experimental Section. Assignment of hydrogens to geminal CH_2 pairs and of these pairs to a bicyclic ring may be easily done using H,H-COSY. The principal problem in making assignments is distinguishing between *exo* and *endo* two-carbon-bridge hydrogens. This distinction is easy in [2.2.1] rings because the ring enforces a significantly smaller bridgehead-*exo* than bridgehead-*endo* dihedral angle. The *exo* coupling is thus

(4) Nelsen, S. F.; Hollinsed, W. C.; Kessel, C. R.; Calabrese, J. C. *J. Am. Chem. Soc.* **1978**, *100*, 7876.
(5) Gerson, F.; Lopez, J.; Akaba, R.; Nelsen, S. F. *J. Am. Chem. Soc.* **1981**, *103*, 6716.
(6) Nelsen, S. F.; Cunkle, G. T.; Evans, D. H.; Haller, K. J.; Kirste, B.; Kurreck, H.; Clark, T. *J. Am. Chem. Soc.* **1985**, *107*, 3289.
(7) Nelsen, S. F.; Kim, Y.; Neugebauer, F. A.; Krieger, C.; Siegel, R.; Kaftory, M. *J. Org. Chem.* **1991**, *56*, 1045.
(8) (a) Nelsen, S. F.; Blackstock, S. C.; Frigo, T. B. *J. Am. Chem. Soc.* **1984**, *106*, 3366. (b) Nelsen, S. F.; Blackstock, S. C.; Frigo, T. B. *Tetrahedron* **1986**, *42*, 1769.

Table II. Summary of NMR, ESR, and ENDOR Data for $6^{\bullet+}$–$9^{\bullet+}$

species	hydrogen, type	δ(n), ppm	δ(c)[0],[a] ppm	$a(H)_{NMR}$, G	$a(H)_{ESR}$, G	$a(H)_{END}$, G
22/**22**$^{\bullet+}$ (**6**$^{\bullet+}$)	exo, x	1.64	unobs		2.87 (8H)[b]	+2.80[c]
(inverting)	endo, n	2.27	–41.8	–0.60	0.59 (8H)	–0.56
	brid, b	2.71	+9.1	+0.09	unobs	unobs
22/**u22**$^{\bullet+}$ (**7**)	13x|14x, xi	1.53	unobs		+5.4 (2H)[b]	+5.32[c]
22 ring	13n|14n, ni	1.84	–57.7	–0.81		*d*
	4x|5x, xo	1.57	52.1	+0.69		+0.76[d]
	4n|5n, no	2.2	–23.0	–0.34		–0.35[d]
	3b|6b, b	2.75	-4.7_5	–0.10		*d*
u22 ring[i]	9v|10v, v	6.49	unobs		+5.4 (2H)	+6.06
	11x|12x, xo	1.28	75.1[c]	+1.00		*d*
	11n|12n, no	2.2	–18.3[c]	–0.28		*d*
	1b|8b, b	3.47	-6.5_3[c]	–0.14		*d*
21/**22**$^{\bullet+}$ (**8**)	4x|5x, xo	~1.53	unobs		3.92 (2H)[e]	+3.98[c]
21 ring[i]	4n|5n, no	1.63	–59.3	–0.83	15.98 (2N)[e]	–0.87[f]
	13a, a	1.27	–142.4	–1.95		–1.82[f]
	13s, s	~2.13	–67.2	–0.94		*f*
	3b|6b, b	3.34	+54.3	+0.69		+0.62[f]
22 ring[i]	9x|10x, xi	1.43	unobs		5.07 (2H)[e]	+5.09[f]
	11x|12x, xo	~1.60	+136.9	+1.83	1.62[e]	+1.53[f]
	9n|10n, ni	1.98	–42.2	–0.60	0.60[e]	*f*
	11n|12n, no	~2.13	–32.8	–0.47		
	1b|8b, b	2.76	+5[g]	+0.03		
21/**u22**$^{\bullet+}$ (**9**)	13a, a	0.65	–78	~–1.07		
21 ring[h,i]	13s, s	2.46	–54	~–0.77		
	4x|5x, xo	1.38	unobs			
	4n|5n, no	1.55	?	?		
	3b|6b, b	3.44	+44	~+0.55		

[a] See Table I footnote *a*. [b] From reference 8, at 297 K in CH_3CN. [c] This work; toluene/trace CH_3CO_2H, 240 K. [d] The (+)0.76-G line pair presumably represents unresolved +0.69-, +1.00-, and –0.81-G splittings, and the (–)0.35-G line pair, unresolved –0.34- and –0.28-G splittings. [e] This work, at 300 K. [f] The –0.87-G ENDOR splitting presumably corresponds to both the –0.94- and –0.83-G splittings measured by NMR, and the +0.62 splitting, to both the +0.69- and –0.60-G NMR splittings. **21**-d_6 material showed ENDOR splittings: G 5.07 (**22** xi), 4.03 (**21** xi), 1.62, and 0.60. [g] Observed by ^{2}H-NMR of the **22**-d_8 material; obscured by protons of diamagnetic material in unlabeled material. [h] Only observed by ^{2}H-NMR of **21**-d_6 material (see text). ESR (this work) at 300 K on **21**-d_6 material: 17.71 (2N), 6.47? (2H, **22** vinyl), 3.54? (2H, **21** xo). [i] Compound with this ring deuterated proved assignment to ring.

larger, allowing assignment of the *exo* hydrogen by an H,H-COSY experiment. Cross peaks were observed in the H,H-COSY of **22**/**u22** for both the W plan ^4J[4n\|5n,13n\|14n] in the **22** ring and the "1.5W" ^6J[4x\|5x,11x\|12x] coupling across the entire molecule, allowing unambiguous assignment of *exo* and *endo* hydrogens of all three dimethylene bridges. The *exo* C[11\|12] hydrogens of **22**/**u22** resonate 0.9 δ upfield of the *endo* hydrogens, making the assignment of the corresponding peaks in **21**/**u22**, where the chemical shift difference is 1.09 δ, unambiguous. *Syn*/*anti* dimethylene bridge assignments in the **22** ring of **21**/**22** were more difficult but were accomplished by reducing **21**/**u22** with D_2. The resulting **21**/**22**-d_2 lacks the 1.43 δ signal of unlabeled material, and the large (geminal) coupling is gone from the 1.98 δ signal, which integrates for 2H; so this pair is the [9\|10] CH_2 group, and as expected on steric grounds, deuterium was introduced from the *exo* face. At a low cut of the COSY of **21**/**22**-d_2, we saw cross peaks for the [9n\|10n],[11n\|12n] W plan coupling, the [1\|8],[11x\|12x] small vicinal coupling, and the [1\|8],[3\|6] non-W ^4J coupling. The substantial upfield shifts for the *exo* hydrogens relative to the *endo* ones at the same carbon in the **22** ring of **21**/**22** (0.7 δ at C[9\|10] and 0.5 at C[11\|12]) allow assignment of the 0.6 δ upfield CH_2 signal of **22**/**22** to the *exo* hydrogens (double nitrogen inversion interconverts the CH_2 carbons without averaging *exo* and *endo* hydrogens). Assignments to *exo* and *endo* dialkyl **21** ring for **21**/**21** were made by using d_6 material prepared from 1,3-cyclopentadiene-d_6.[9]

Small errors in δ(n), δ for the neutral compound, do not influence a(H) for the radical cation determined by NMR significantly, because a change of 0.7 δ only changes a(H) by 0.01 G (see eq 2). Values for δ(n) were inferred from compounds for which accurate assignments have been made for compounds for which complete assignments are not given in the Experimental Section.

(9) Nelsen, S. F.; Frigo, T. B.; Kim, Y.; Thompson-Colon, J. A.; Blackstock, S. C. *J. Am. Chem. Soc.* **1986**, *108*, 7926.

Sesquibicyclic Hydrazine Radical Cation a(H) Values. The a(H) values determined by NMR, ESR, and ENDOR for **22**/**22**$^{\bullet+}$ and **22**/**u22**$^{\bullet+}$ (**6**$^{\bullet+}$ and **7**$^{\bullet+}$) appear in Table II. Double nitrogen inversion is rapid, so only three spittings are present for **22**/**22**$^{\bullet+}$. The especially small bridgehead splitting could only be observed by NMR, but as expected, the large *exo* splitting was not observed. The dissymmetry introduced by the unsaturation produces nine different splittings for **22**/**u22**$^{\bullet+}$, but the complexity

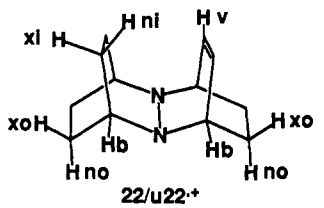

22/**u22**$^{\bullet+}$

of the spectrum and small size of several splittings led to observation of only two of the seven <2-G splittings by ENDOR, which is insufficient to allow assignments. The ^{1}H-NMR spectrum of a nearly saturated solution of **22**/**u22**$^{\bullet+}$ is shown in Figure 1. In addition to two pairs of overlapping signals near –5 (labeled A and B) and –20 (C and D) δ, there are very broad signals at about –55 (E) and +55 (G) δ which cannot be clearly distinguished from baseline roll (caution: proper baseline corrections can only be made after high total radical concentration spectra are obtained; in our early work we "lost" the positive δ peak labeled G entirely in attempting to make the baseline "correction"). Figure 2 shows the spectrum at 81 mM after the addition of 541 mM **1**. The signal for **1** at ~–5 δ obscures the A and B signals at ~–5 δ but sharpens the other peaks substantially and reveals the signal corresponding to the seventh small splitting (labeled F). The predominant invertomer is that illustrated. We use outer and inner to refer to the bridges directed away from and toward the center of the molecule in the predominant

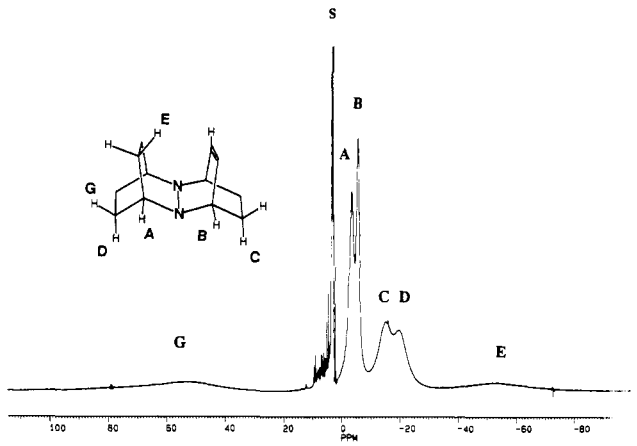

Figure 1. ^{1}H-NMR spectrum of a 218 mM solution of **22/u22**$^{\bullet+}$ (**7**$^{\bullet+}$) in CD_3CN. Final assignments (see text) are shown on the structure.

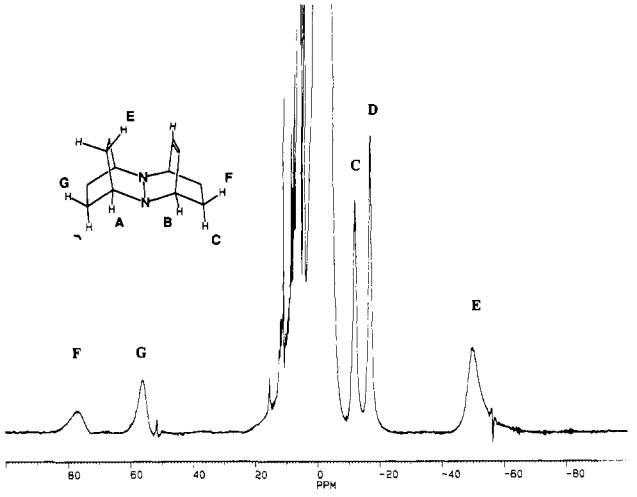

Figure 2. ^{1}H-NMR spectrum of an 81 mM solution of **22/u22**$^{\bullet+}$ (**7**$^{\bullet+}$) in CD_3CN after the addition of 541 mM **1**. Final assignments (see text) are shown on the structure.

invertomer and *exo* and *endo* to refer to the diastereomeric hydrogens on two carbon bridges; xi hydrogens are in W plan with the spin-bearing 3e-π NN system and have a(H) too large to observe by NMR. When the invertomers are similar enough in energy, both $a(H_{xi})$ and $a(H_{xo})$ are large. For **22/22**$^{\bullet+}$ the two invertomers are equal in energy by symmetry, and only one x splitting is present. Three pairs of small splittings of similar size, which ought to correspond to xo, no, and b splittings because these hydrogens are geometrically very similar in both the **22** and **u22** rings, are observed for **22/u22**$^{\bullet+}$. The seventh small splitting observed lacks a partner and can be directly assigned to the **22** ring ni hydrogen. Study of the d_8 species prepared from 1,3-cyclohexadiene-d_8 allowed assignment of each pair of splittings to the proper ring. The smallest splittings are clearly those of the bridgehead hydrogens, securely assigned to the smallest splitting of **22/22**$^{\bullet+}$ from the ESR spectrum. The remaining assignment, between xo and no, requires more consideration. The average of the no and ni splittings should be close to the –0.60-G splitting of **22/22**$^{\bullet+}$, and the choices are –0.58 (the assignment given) and –0.06 G (if the xo and no assignments were switched). The averge of the xi and xo splittings should be close to the 2.87-G x splitting of **22/22**$^{\bullet+}$, and the choices are 3.00 (assignment given) and 2.49 G. W plan splittings increase as N pyramidality increases, also in agreement with the assignment. Both the W and non-W *exo* splittings are positive, but all three *endo* splittings are negative.

21/22$^{\bullet+}$ (**8**$^{\bullet+}$) showed eight NMR signals, and ENDOR demonstrated that the two missing signals correspond to splittings too large to observe by NMR; +5.09 G for the **22** ring xi splitting and 3.98 G for the **21** ring xo splitting. Study of the **21**-d_6 material allowed assignment of the observed splittings to the bicyclic ring. Qualitatively the **22** ring splittings are as expected, a small b splitting, a positive xi splitting, and two small negative n splittings. The only positive small splitting in the **21** ring is assigned as the b splitting, which is considerably larger than that for **22** rings, as expected (see below). The ni splitting is negative, in agreement with negative n splittings for **22/u22**$^{\bullet+}$, as are the *syn* and *anti* splittings at the one-carbon bridge, which lie in the nodal plane of the 3e-π bond at the nitrogens. Integration is unreliable for NMR spectra of radicals due to severe baseline instability; but for the ^{2}H-NMR of the **21**-d_6 material, the –60.9 and –143.7 δ signals were clearly about half the intensity of the other two, and we assign them to the C(13) hydrogens, with the larger splitting assumed to be *anti*.

Table III. Summary of NMR and ESR Data for **10**$^{\bullet+}$ and **11**$^{\bullet+}$

species	hydrogen type	δ(n), ppm	δ(c)^0,[a] ppm	a(H)$_{NMR}$, G
21/21$^{\bullet+}$ (**10**$^{\bullet+}$)[b]	4x|9x, x	1.35	unobs	
(inverting)	4n|9n, n	1.49	–53.2	–0.74
	1b|3b, b	3.34	+28.9	+0.35
	11a|12a, a	1.86	–147	–2.01
	11s|12s, s	1.21	–73.4	–1.02
21/23$^{\bullet+}$ (**11**$^{\bullet+}$)[c]	4x|5x, xo	(1.5)		
21 ring[e]	4n|5n, no	(1.6)	–60.3[d]	–0.84
	14a, a	(1.3)	–166	–2.27
	14s, s	(2.1)	–79.4	–1.10
	3b|6b, b	(3.3)	+65.8	+0.84
23 ring	12x|13x, xi	(2.2)		
	12n|13n, ni	(1.7)	–33	–0.47
	9s|11s, 3s	(1.7)	+74.4	+0.99
	9a|11a, 3a	(1.9)	–60.3[d]	–0.84
	1b|8b, b	(2.9)	+4.5	+0.02

[a] See Table I footnote *a*. [b] a(H)$_{ESR}$ from d_{12} material containing only x protons = 4.2 G.[9] At low temperature, xi 6.85, xo 1.4 G, proving that both are positive.[9] [c] See text. We presume the splittings at C(10) are too small to observe. [d] Both the **21** and **23** rings have signals near –60 ; which are not resolved. [e] Assignment made with this ring deuterated.

21/u22$^{\bullet+}$ (**9**$^{\bullet+}$) proved especially difficult to study. It reacts with **1**, and only one peak could be discerned in the NMR of unlabeled material. The three peaks reported in Table II are from the ^{2}H-NMR of a saturated solution of **21**-d_6-labeled **9**$^{\bullet+}$, and although the splittings obtained are clearly less accurate than those for the systems for which dopant could be used, the shifts are consistent with those obtained for the **21** ring of **8**$^{\bullet+}$. It seems likely that both no and *syn* hydrogens contribute to the peak observed at –78 ppm. Clear ENDOR peaks were not observed.

21/21$^{\bullet+}$ (**10**$^{\bullet+}$) is equilibrating between equal-energy nitrogen inversion forms at 300 K. The two large negative splittings which differ by about a factor of 2 are assigned to *anti* and *syn*, the remaining negative splitting to n, and the small positive splitting to b, in agreement with assignments previously made for **21** rings. Published dynamic ESR studies demonstrate that the x splitting is too large to be observed by NMR and that xi and xo are both positive (see Table III).[9] As for **21/u22**$^{\bullet+}$, clear ENDOR peaks were not observed, which might be caused by dynamic line broadening for these compounds.

21/23$^{\bullet+}$ (**11**$^{\bullet+}$) appeared to show only seven of the ten smaller splittings expected (the xi splitting in the **23** ring and xo splitting in the **22** ring should be too large to observe). Study of the **21**-d_6 material demonstrated that the –60.3 δ signal had contributions both from the **23** ring (it was present in the ^{1}H-NMR) and from the **21** ring (it was present in the ^{2}H-NMR as well). Small splittings are expected for the *syn* and *anti* hydrogens at C(10), which are δ to N and also lie in the nodal plane of the 3e-π bond at N, and we presume that the two missing signals correspond to these hydrogens. A peak possibly corresponding to one or

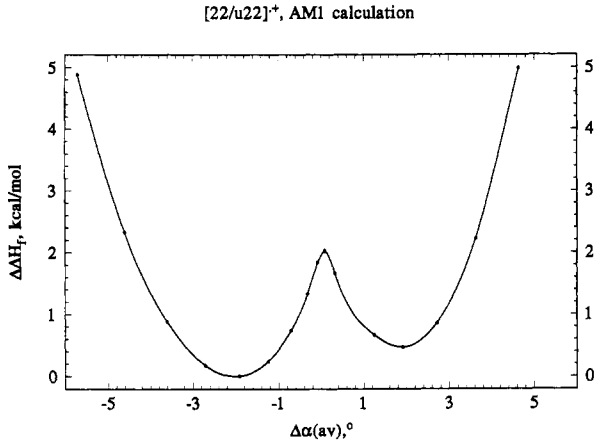

Figure 3. Energy surface for **22/u22**•+ (**7**•+) calculated by AM1-UHF.

both C(10) hydrogens was observed at +1.4 δ in the ^{1}H spectrum of the **21**-d_6 material, but it could also arise from a diamagnetic impurity.

Assignments to bicyclic ring by deuteration were not made for **12**•+–**14**•+, and assignments made by analogy appear in the Experimental Section.

Discussion

Sesquibicyclic Hydrazine Radical Cation Energy Surfaces. Interpretation of a(H) values for radicals is complicated by the fact that energy surfaces for geometry change are usually rather flat and a weighted average over a range of geometries which have significantly different a(H) values is in fact contributing to the observed value. This range of geometries is severely limited for the compounds discussed here by the presence of two bicyclic rings fused at the nitrogens, but all compounds studied have nonplanar nitrogens, with two invertomers occupied. We shall call the most stable conformation A and its invertomer B for convenience. Pyramidality at nitrogen is best considered by using the average of the three heavy-atom bond angles at nitrogen, because this quantity is almost linear with fractional p hybridization (and hence with orbital energy) in the range considered.[9,10] In this discussion we shall describe nitrogen pyramidality by $\Delta\alpha_{av} = 120 - \alpha_{av}$, which varies from 0 for a planar nitrogen to 10.5° for a tetrahedral one. AM1 calculations have been shown to give an optimized structure with $\Delta\alpha_{av}$ about right for **22/u22**•+ and to calculate the double nitrogen inversion barrier for **21/21**•+ rather well.[9,10] The AM1-calculated energy surface for **22/u22**•+ is shown as Figure 3 and is close to two intersecting parabolas displaced by $\Delta\Delta H_f$ for the invertomers. Results of AM1 calculations for the species studied here are summarized in Table IV, along with the fraction of the major conformation present, f_A, estimated from the calculations by assuming that $\Delta G° = \Delta\Delta H_f$. A major question we hoped to be able to answer by measuring the hydrogen splittings is what f_A actually is for these species. The hydrogen splitting expectation values depend strongly upon f_A, and it is so sensitive to the A, B energy separation that there is no hope that calculations could give f_A values accurately enough to test the ability of calculations to properly estimate splitting constants. In this paper we try to determine f_A as accurately as possible.

Bridgehead Splittings. The bridgehead splittings of these hydrazine radical cations are rather far from what would be anticipated using the usual β-splitting formula shown as eq 3:

$$a(H_\beta) = (A + B\langle\cos^2\theta_b\rangle)\rho_N^\pi \qquad (3)$$

θ_b is the twist angle between the axis of the π (rich) orbital at N and the C–H_b bond, and ρ_N^π is the π spin density at N. A methyl group has $\langle\cos^2\theta_b\rangle = 0.5$, and a(Me) for 2,3-dimethyl-2,3-diazabicyclo[2.2.2]octane is 12 G;[10] so because A is $\ll$ B, $B\rho_N^\pi$ is ~24 G. θ_b at given $\Delta\alpha_{av}$ values is known rather well for these systems because their tetracyclic structures limit available geometries. The entries for θ_b in Table V are calculated assuming that the lone pair bisects the CNN angle in a Newman projection down the C_b–N bond at the AM1 optimized geometry of each invertomer. According to eq 3, A would have to be unusually negative (ca. –3.2 G, using the 75° θ_b from the equilibrium AM1 structure in Table V) to make the bridgehead splitting as small as that observed for **22/22**•+, which has $\Delta\alpha_{av}$ = 1.9° by AM1 and 1.8 and 1.1 for two different molecules in a rather poorly determined X-ray structure.[9b] The same A and B obviously could not be used for **21/21**•+, which is predicted to have a bridgehead splitting on the order of 14 times larger than that observed. We do not think that the θ_b values from Table V are likely to be significantly wrong; but the $\cos^2\theta_b$ relationship only holds exactly for a pure p orbital, and significant deviations from it are expected as the nitrogen pyramidalizes. Furthermore, the bridgehead hydrogens are γ to a nitrogen of opposite spin as well as β to the nitrogen to which θ_b refers. We suggest that the small bridgehead splittings observed for sesquibicyclic hydrazines are caused by significant γ as well as β nitrogen contributions to $a(H_b)$ and that eq 3 is not useful for quantitative estimation of θ_b for these compounds.

For all but **22/22**•+ and **21/21**•+, where $\Delta\Delta H_f$ is zero by symmetry, the energy difference between invertomers is unknown. The f_A entries in Table V are those given by the $\Delta\Delta H_f$ values,

(10) Nelsen, S. F.; Frigo, T. B.; Kim, Y. *J. Am. Chem. Soc.* **1989**, *111*, 5387.

Table IV. AM1-Calculated Double N Inversion Minima for Sesquibicyclic Hydrazines

compound	$\Delta\alpha_{av}$ values: α	B	$\Delta\Delta H_f$(B–A), kcal/mol	calc f_A[a]
22/23•+ (**12**•+)	1.0	1.5	0.15	0.56
22/u23•+ (**13**•+)	1.5	1.0	0.30	0.63
u22/23•+ (**14**•+)	1.6	1.0	0.44	0.68
22/22•+ (**6**•+)	1.8	1.8	≡0	0.50
22/u22•+ (**7**•+)	2.0	1.9	0.47	0.69
21/23•+ (**11**•+)	2.3	1.0	0.69	0.74
21/22•+ (**8**•+)	2.9	2.2	0.06	0.53
21/u22•+ (**9**•+)	2.9	2.2	0.78	0.79
21/21•+ (**10**•+)	3.9	3.9	≡0	0.50

[a] At 25 °C, assuming $\Delta G° = \Delta\Delta Hf$, where A is the calculated most stable N invertomer form.

Table V. Comparison of Observed Bridgehead Splittings with AM1-Calculated θ_b and Conformational Fractions for Sesquibicyclic Hydrazine Radical Cations

compound[a]	$a(H_b)$, G	AM1 energy minima: θ_b, deg (f_A or f_B[b])
22/**23**•+ (**12**•+)	+0.02	80(0.56), 78(0.44)
22/**u23**•+ (**13**•+)	+0.14	78(0.63), 80(0.37)
22/**22**•+ (**6**•+)	+0.09	75(≡0.5), 75(≡0.5)
22/**u22**•+ (**7**•+)	–0.10	77(0.69), 76(0.31)
21/**22**•+ (**8**•+)	+0.03	72(0.53), 74(0.47)
22/**u22**•+ (**7**•+)	–0.14	77(0.69), 76(0.39)
u22/**23**•+ (**14**•+)	–0.04(?)	79(0.68), 78(0.32)
21/**23**•+ (**11**•+)	+0.84	94(0.74), 61(0.26)
21/**22**•+ (**8**•+)	+0.69	92(0.53), 55(0.47)
21/**u22**•+ (**9**•+)	+0.55	91(0.79), 56(0.21)
21/**21**•+ (**10**•+)	+0.35	87(≡0.5), 50(≡0.5)
22/**23**•+ (**12**•+)	+0.21(?)	67(0.56), 90(0.44)
u22/**23**•+ (**14**•+)	+0.20(?)	90(0.68), 67(0.32)
21/**23**•+ (**11**•+)	+0.02(?)	87(0.74), 66(0.26)
22/**u23**•+ (**13**•+)	+0.21(?)	93(0.63), 64(0.37)

[a] Underlined ring is the one containing the bridgehead hydrogen to which the entry refers. [b] Fractions of conformation present calculated at 25 °C assuming $\Delta G° = \Delta\Delta H_f$.

Table VI. Saturated Two-Carbon-Bridge Splittings for Sesquibicyclic Hydrazine Radical Cations

compound[a]	*exo* splittings[b]	*endo* splittings
22/**22**$^{\bullet+}$ (**6**$^{\bullet+}$)	+2.87, +2.87	−0.60, −0.60
22/**23**$^{\bullet+}$ (**12**$^{\bullet+}$)	+2.85, 2.68	−0.48 (or −0.74), −0.62
22/**u23**$^{\bullet+}$ (**13**$^{\bullet+}$)	+4.24, +1.63	−0.75 (or −0.82), −0.43
22/**u22**$^{\bullet+}$ (**7**$^{\bullet+}$)	+5.32, +0.69	−0.81, −0.34
21/**22**$^{\bullet+}$ (**8**$^{\bullet+}$)	+5.09, +1.83	−0.60, −0.47
22/**u22**$^{\bullet+}$ (**7**$^{\bullet+}$)	+1.00	−0.28
u22/**23**$^{\bullet+}$ (**14**$^{\bullet+}$)	+1.56 (or +0.57)	−0.30
21/**23**$^{\bullet+}$ (**11**$^{\bullet+}$)		−0.84
21/**22**$^{\bullet+}$ (**8**$^{\bullet+}$)	+3.98	−0.83
21/**u22**$^{\bullet+}$ (**9**$^{\bullet+}$)		−0.77(?)
21/**21**$^{\bullet+}$ (**10**$^{\bullet+}$)	+4.2 (6.85, 1.4)	−0.74
22/**23**$^{\bullet+}$ (**12**$^{\bullet+}$)	+2.22	−0.74 to −0.47
u22/**23**$^{\bullet+}$ (**14**$^{\bullet+}$)		−0.57 or −0.68
23/**21**$^{\bullet+}$ (**11**$^{\bullet+}$)		−0.47

[a] Underlined ring is the one containing the hydrogens to which the entry refers. [b] Underlined splittings are from ENDOR or ESR.

assuming $\Delta\Delta S$ is zero. When θ_b values differ significantly for invertomers, as for cases having **21** and **23** rings, estimated $a(H_b)$ depends significantly on the energy difference between invertomers. The AM1-calculated values cannot all be correct. For example, AM1 gets the result that **22**/**23**$^{\bullet+}$ has the 3 and 2 bridges *syn* in the more stable conformation (making $\theta_b \sim 67°$), but **u22**/**23**$^{\bullet+}$ has the 2 and unsaturated 2 bridges *syn* (making $\theta_b \sim 90°$). This turnaround in preferred conformation clearly does not occur, because significantly larger $a(H_b)$ values would have been observed for the former compound. Another case where the AM1 energy difference between double N inversion isomers appears qualitatively wrong occurs for **21**/**22**$^{\bullet+}$, which ought to have shown significantly larger $a(H_b)$ if the small θ_b conformation really were a much larger contributor than those for the other **21** compounds studied.

Dimethylene Bridge Splittings. The observed splittings for *exo* and *endo* hydrogens of the two-carbon bridges studied are summarized in Table VI. Inversion at the nitrogens exchanges the inner and outer carbons of the **22** ring, and W plan splittings are clearly larger than non-W ones. For compounds containing both a **22** ring and an unsymmetrical ring, the invertomers are different in energy. The xo splitting should decrease from the 2.87 (room temperature) value observed for **22**/**22**$^{\bullet+}$ as f_A increases from 0.5. One might hope to be able to use the *exo* splittings in the **22** ring to measure the equilibrium constant for double N inversion. It should be noted that both ENDOR and NMR measurements are required for obtaining both the $a(H_{xi})$ and $a(H_{xo})$ values required to do this for our compounds. For **22**/**u22**$^{\bullet+}$ the two *exo* splittings observed for the **22** ring are

$$a(H_{xi}) = 5.32 = f_A A_{WA} + (1 - f_A)A_{NB} \quad (4)$$

$$a(H_{xo}) = 0.69 = (1 - f_A)A_{WB} + f_A A_{NA} \quad (5)$$

A and B for this compound are illustrated below, along with

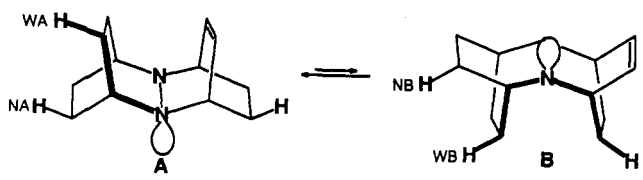

indentification of the splitting constants used in eqs 4 and 5. Because of the local symmetry of the **22** ring and the similarity of predicted $\Delta\alpha_{av}$ values for the two invertomers (Table IV), one might hope to be able to use the same splitting constants A_W and

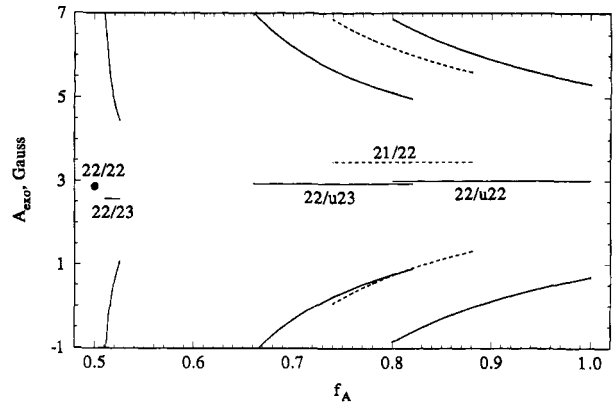

Figure 4. Plot of W and non-W plan *exo* **22** ring hydrogen splittings as a function of f_A calculated using eqs 4–7.

A_N for the W plan and non-W plan splittings in both invertomers, as indicated in eqs 6 and 7. Assuming eqs 6 and 7, $a(H_{xo}) +$

$$A_{WA} = A_{WB} = A_W \quad (6)$$

$$A_{NA} = A_{NB} = A_N \quad (7)$$

$a(H_{xi}) = A_W + A_N$. **22**/**22**$^{\bullet+}$ has $f_A = 0.5$ by definition, and its observed *exo* splitting of 2.87 G is therefore $(A_W + A_N)/2$. Figure 4 shows plots of A_W and A_N obtained from eqs 4–7 as a function of f_A for the other four compounds having **22** rings. The 200 K ENDOR spectrum of **22**/**23**$^{\bullet+}$ shows very similar *exo* splittings for all three dimethylene bridge hydrogens. Choosing the two largest, which average to 2.77 G, as those in the **22** ring only allows a very narrow range near 0.51 for f_A, as indicated in Figure 4 and shown numerically in Table VIIa. A_W for the **22** ring of these systems is expected to increase as nitrogen pyramidality increases, and we believe it must be less than the 6.85 G which has been directly measured for the dimethylene bridge of **21**/**21**$^{\bullet+}$ at low temperature.[9] It must be larger than the 5.32 G observed for $a(H_{xi})$ of **22**/**u22**$^{\bullet+}$ and can only be close to this number if f_A for this compound is close to 1. We therefore suggest that f_A can only reasonably be in the ranges obtained using A_W in the 5.5–6.25 range appearing in Table VII for **22**/**u22**$^{\bullet+}$, **22**/**23**$^{\bullet+}$, and **22**/**u32**$^{\bullet+}$. We doubt that eqs 6 and 7 can hold quantitatively as the second bicyclic ring becomes increasingly asymmetrical. Although the data for **21**/**22**$^{\bullet+}$ are included for comparison both in Figure 4 (as the dotted curves) and in Table VIIa, the significantly deviating curves of Figure 4 and the significantly larger average $a(H_{exo})$ of Table VII indicate that eqs 6 and 7 are probably no longer very good assumptions and that the f_A values calculated assuming them are unlikely to be as reliable as those for the other compounds. The sum $S = a(H_{xi}) + a(H_{xo})$ changes as shown in Table VII. Because A_W should increase as pyramidality at N increases, this is expected, but it suggests that eqs 6 and 7 may not be as good approximations as one might be able to make even for **22**/**u23**$^{\bullet+}$ and **22**/**u22**$^{\bullet+}$. The expected S increase because A_{WA} increases as pyramidality increases was quantitated employing eq 8, that is that a second

$$A_{WA} = RA_{WB}, \text{ where } R = 1 + (S - 5.74)/(f_A A_W) \quad (8)$$

approximation to estimating f_A from the experimental spectra might be usefully obtained by using a larger A_W for the more nitrogen pyramidal A form than for the less pyramidal B form. Using f_A and A_W pairs from estimations assuming eqs 6 and 7 produces quite constant R values (Table VIIb). Because A_{NA} and A_{NB} also probably change with pyramidality, there are more unknowns than equations, so analytical calculation of f_A cannot be carried out. Nevertheless, using eq 8 with eqs 4 and 5 causes the "second approximation" f_A estimate (called f_A' in Table VIIb)

Table VII. Conformational Populations Estimated from *Exo* **22** Ring Splittings

compound	**22/22**$^{\bullet+}$ (**6**$^{\bullet+}$)	**22/23**$^{\bullet+}$ (**12**$^{\bullet+}$)	**22/u23**$^{\bullet+}$ (**13**$^{\bullet+}$)	**22/u22**$^{\bullet+}$ (**7**$^{\bullet+}$)	**21/22**$^{\bullet+}$ (**8**$^{\bullet+}$)
$a(H_{xi})$, G	(2.87)	2.85	4.24	5.32	5.09
(H_{xo}), G	(2.87)	2.68	1.63	0.69	1.83
$a(H_{xi}) + (H_{xo})$	5.74	5.53	5.87	6.01	6.92
a. Assuming Eqs 4–7 May be Employed					
$f_A(A_N)$if A_W = 5.50	≡0.5	0.516(+0.02)	0.75(+0.37)	0.96(+0.51)	0.90(+1.42)[a]
if A_W = 6.25		0.512(–0.72)	0.70(–0.38)	0.86(–0.24)	0.70(+0.67)[a]
$\Delta G°$ (25 °C), kcal/mol	≡0.0	0.035 ± 0.005	0.6 ± 0.1	1.5 ± 0.4$_5$	*a*
b. Assuming Eqs 4, 5, and 8					
R (see eq 8)			1.03	1.05	1.24
A_{WA}, G			5.9 ± 0.3	6.1 ± 0.2	6.8 ± 0.2
A_{NB}, G			0.5 ± 0.5	0.5 ± 0.5	1 ± 1
A_{NA}, G			2.4 ± 0.2	0.8 ± 0.04	2.6 ± 0.3
f_A'			0.69 ± 0.07	0.86 ± 0.05	0.70 ± 0.08[b]
$\Delta G°$(25 °C), kcal/mol			0.5 ± 0.2	1.1 ± 0.3	0.5 ± 0.2
$\Delta\Delta H_f$ (by AM1)	≡0.0	–0.15	0.30	0.47	0.06

[a] Equations 6 and 7 are unlikely to apply very quantitatively (see text). [b] For the **21** ring, using A_{WB} = 6.8 ± 0.2 G and A_{NA} = 2.2 ± 0.2 in eq 5 gives f_A = 0.67 ± 0.05.

to be increasingly lower than estimates from eqs 4–7 as *R* increases. We suggest that these f_A' values are the best estimates we are able to make of f_A for these systems. In summary, the B, A $\Delta G°$ for **22/23**$^{\bullet+}$ is indicated by its *exo* splitting constants to be about 0.2 kcal/mol different from the AM1 $\Delta\Delta H_f$ difference (Table VIIa; assuming that AM1 got the wrong conformation as A; the energy difference is tiny), while the $\Delta G°$ difference for **22/u22**$^{\bullet+}$ and **21/22**$^{\bullet+}$ is about 0.6 and 0.4 kcal/mol higher than the AM1 $\Delta\Delta H_f$ difference (Table VIIb). Although the AM1 calculations make only rather small errors in relative energy, the sensitivity of the ESR spectrum to f_A both makes it important to know f_A to estimate the averaged splitting and provides a sensitive probe for its value.

Despite the geometrical similarities of the **22** and **u22** rings at their CH_2CH_2 bridges, $a(H_{xo})$ in the **u22** ring of **22/u22**$^{\bullet+}$ is +1.00 G, about 45% larger than $a(H_{xo})$ in the **22** ring, although f_A is the same by definition. The weighting of the A_{NA} contribution is considerably larger than that of the A_{WB} contribution to $a(H_{xo})$ (eq 5), which suggests that the non-W γ splitting constant A_{NA} is significantly more positive for the unsaturated ring, which has allylic N_α–C_β and C_β–C_γ bonds, than it is in the saturated ring.

The *endo* splittings (Table VI) are not very sensitive to structure and convey little conformational information. The same is true for the **21** ring *anti* and *syn* methylene bridge hydrogens, for which the splittings obtained are **21/21**$^{\bullet+}$ –2.01, –1.02; **21/22**$^{\bullet+}$ –1.95, –0.94; **21/u22** unobs, –1.07; **21/23**$^{\bullet+}$ –2.27, –1.10 (the more negative splitting was assumed to be the *anti* one in calculating $\Delta\delta$).

Conclusions

The NMR method has significantly better resolution than ENDOR for small splitting constants, but ENDOR measurements are necessary for splitting constants over 2 G if many small splittings are present so that the ESR spectrum is complex. Bridgehead splittings in sesquibicyclic hydrazines are positive for **21** rings, smaller and positive for **23** rings, and very small for **22** rings. There is not, however, a simple relationship with $\cos^2\theta_b$, apparently because of significant effects from the nonadjacent nitrogen. *Exo* splittings for dimethylene bridges in sesquibicyclic hydrazines show positive splittings for the cases investigated, are much larger for hydrogens in W plan with the nitrogen lone pair orbitals than for non-W hydrogens, and appear to be very sensitive to nitrogen pyramidality. Examination of the *exo* splitting constants shows that energy differences between the invertomers of **22/u22**$^{\bullet+}$ and **22/u23**$^{\bullet+}$ are underestimated by a few tenths of a kcal/mol by AM1.

Experimental Section

Materials. Preparations of **2**,[4] **3**,[11] **4**,[6] **5**,[7] **6** and **7**,[8a] **8**, **9** and **11**,[8b] **10**, **12**, and **13**[9] were reported previously, and oxidation to their radical cations was carried out with $NOPF_6$, as previously described.[9,10]

1,3-Cyclohexadiene-d_8. A solution of 360 mg of potassium *tert*-butoxide in 10 mL of DMSO-d_6 was added to 2.37 mL of 1,3-cyclohexadiene in 20 mL of pentane under N_2; the two-phase mixture was stirred vigorously for 2 h, and the DMSO layer was removed by syringe. After treatment with a fresh potassium *tert*-butoxide/DMSO-d_6 solution for 2–10 h, the pentane layer was separated, washed with 2 × 25 mL of water and with 25 mL of saturated sodium chloride solution, dried over magnesium sulfate, and concentrated. The resulting mixture of deuterated 1,3- and 1,4-cyclohexadienes was separated by preparative GC on a 10-ft Apiezon L column.

2,8-Diazatetracyclo[7.2.2.2^{3,7}.0^{2,8}]pentadeca-14-ene (14). A solution of 2.04 g (18 mmol) of 2,3-diazabicyclo[2.2.2]oct-2-ene was treated with 3.60 g (19 mmol) of 85% HBF_4·Et_2O, and the supernatant was removed by cannula from the white salt formed after 5 min. The salt was washed with 3 × 100 mL of ether and dried by blowing N_2 over it for 3 h. After solution in 100 mL of acetonitrile, 2.5 mL (23 mmol) of 1,3-cycloheptadiene in 50 mL of acetonitrile was added by syringe; and after the reaction mixture was stirred at 45 °C under N_2 for 102 h, an additional 1.0 mL (9 mmol) of 1,3-cycloheptadiene was added, and the solution was stirred an additional 40 h at 45 °C under N_2. The volume was reduced to 30 mL under vacuum, 150 mL of ether was added slowly, and the yellow precipitate was gathered, washed with ether (4 × 100 mL), and dried in vacuum, giving 3.72 g (68.9%) of crude **14**·HBF_4. A mixture of 1.04 g (3.56 mmol) of this material and 10 g of powdered sodium hydroxide in 50 mL of dry ether was vigorously stirred for 5 h at room temperature, filtered through Celite, and concentrated. The product was recrystallized from ether at –78 °C to yield 0.634 g (87%) of **14** as a white solid, mp 55–56 °C. ^{1}H-NMR: (500 MHz, $CDCl_3$) δ 1.28 (ddt, H[10a′eq′]), 1.51 (m, H[14n|15n]), 1.54 (m, H[10s′ax′]), 1.59 (m, H[3x|4x]), 1.72 (m, H[9a|11a]), 1.75 (m, H[9s|11s]), 1.91 (m, H[14n|15n]), 2.11 (m, H[4n|5n]), 2.70 (br s, H[3b|6b]), 3.27 (br s, H[1b|8b]), 6.25 (AA′ of AA′BB′, H[12v|13v]). ^{13}C-NMR (125.56 MHz, $CDCl_3$) δ 19.24, 24.77, 28.43, 31.95, 54.24, 58.35, 128.64. HRMS calcd for $C_{13}H_{20}N_2$ 204.1626, found 204.1625.

NMR spectra of neutral hydrazines were run on Brucker WP-200, WP-270, or AM-500 MHz instruments. Assignments mostly relied on H,H-COSY experiments. **6 (222/222)** ^{1}H-NMR (200 MHz, CD_3CN) δ 2.71 (4H[bridgehead]), 2.27 (8H[*endo*]), 1.64 (8H[*exo*]). **7 (222/u222)** ^{1}H-NMR (500 MHz, $CDCl_3$) δ 6.49 (2H[9|10]), 3.47 (2H[1|8]), 2.75 (2H[3|6]), ~2.2 (2H[4n|5n] *overlaps with* 2H[11n|12n]), 1.84 (2H[13n|14n]), 1.57 (2H[4x|5x]), 1.53 (2H[13x|14x]), 1.28 (2H[11x|12x]). ^{13}C-NMR (125 MHz, $CDCl_3$; assignments made by C,H correlation spectroscopy) 130.1 [9|10], 54.6 [1|8], 51.1 [3|6], 29.7 [11|12], 25.9 [4|5], 25.6 [13|14]. **8 (221/222)** ^{1}H-NMR (500 MHz, $CDCl_3$) δ 3.34 (2H[3|6]), 2.76 (2H[1|8]), ~2.13 (2H[11n|12n] *overlaps with* 1H[13s]), 1.98

(11) Nelsen, S. F.; Kessel, C. R.; Brien, D. J. *J. Am. Chem. Soc.* **1980**, *102*, 702.

(2H[9n|10n]), 1.63 (2H[4n|5n]), ~1.60 (2H[11x|12x]), ~1.53 (2H[4x|5x]), 1.43 (2H[9x|10x]), 1.27 (1H[13a], d, J = 12.5 Hz). ^{13}C-NMR (125 MHz, $CDCl_3$) 61.3 [3|6], 49.5 [1|8], 34.1 [13], 32.1 [4|5 *or* 11|12], 28.8 [11|12 *or* 4|5], 21.5 [9|10]. **9 (221/u222)** ^{1}H-NMR (500 MHz, $CDCl_3$) δ 6.34 (2H[9|10]), 3.59 (2H[1|8]), 3.44 (2H[3|6]), 2.46 (1H[13s], d of apparent quint, J = 10, 2.4 Hz), 2.01 (2H[11n|12n]), 1.55 (2H[4n|5n]), 1.38 (2H[4x|5x]), 1.12 (2H[11x|12x]), 0.65 (1H[13a], d, J = 10.0 Hz). **10 (221/221)** ^{1}H-NMR (500 MHz, $CDCl_3$) δ 3.57 (2H[1|8]), 3.41 (2H[3|6]), 2.28 (1H[11s]), 1.92 (1H[12s]) overlaps with 1.90 (2H[9n|10n]), 1.54 (2H[4x|5x]), ~1.46 (1H[11a]) overlaps with ~1.46 (2H[4n|4n]), 1.41 (2H[9x|10x]), 1.20 (1H[12a], d, J = 10.8 Hz).

ESR, ENDOR, and triple-resonance spectra were measured using a Brucker ESP 300 spectrometer equipped with the ER(ENMR)ENDOR system.

NMR Spectra of Hydrazine Radical Cations. A. Method. All spectra were acquired on an unmodified Bruker AM-500 spectrometer equipped with a 5-mm proton probe at a constant temperature of 300 K. A sweep width of 166 KHz, size of 16 K, pulse width of 2.5 μs, and receiver delay of 1 s were employed. A spectrum of neat CD_3CN was run prior to each sample, and the methyl resonance was set to 1.93 ppm; it is essential that the radical cation spectrum recorded have the same lock field and SR value as this external standard. ^{2}H spectra were recorded using the same spectrometer with a 5-mm BB probe, which had a background ^{1}H signal and could not be used for ^{1}H spectra.

Samples were prepared by dissolving 6–60 mg of desired radical cation in 400 μL of CD_3CN which had been deaerated with Ar, using a nitrogen-filled glovebag and "no-air" septum to cap the 5-mm NMR tube. After an initial spectrum was obtained, **1** was added in 10–20-μL aliquots until a total radical concentration (radical cation plus **1**) near 1 M was reached. The resulting spectra were Fourier transformed (with line broadening of 20 Hz) and baseline corrected using a spline fit in reverse order (higher concentration first), to minimize the possibility that very broad resonances would be lost due to the baseline correction. Plots of δ(c) vs total radical concentration were extrapolated to zero concentration to give the $\delta(c)^0$ values in Tables I–III. Due to the insensitivity of the ^{2}H signal and high number of scans required, **1** was added in 20–50-μL aliquots and fewer total spectra were required. These spectra did not suffer from the extreme baseline roll seen in the ^{1}H spectrum, but insensitivity makes acquisition of useful ^{2}H spectra more difficult than that of ^{1}H spectra.

B. 222/322$^{\bullet+}$ (12). ESR (300 K): G 14.06 (2N). ENDOR (200 K): G +2.85 (222 xi), +2.68 (222 xo), +2.22 (322), +0.84. NMR: Eight of the 12 different hydrogen splittings are seen: δ +78.6, +63.9, +18.4, +4.3; –33, –43.9, –44.2, –52.7. We presume that the two missing ones are at the [322] methylene on the node. Assignments based on analogy: *222 ring:* 14x|15x, unobs; 4x|5x, unobs; 14n|15n, –43.9/–44.2; 4n|5n, –52.7; 3b|4b, +4.3/+18.4. *322 ring:* 12x|13x, unobs; 12n|13n, –33; 9s|11s, +63.9/+78.6; 9a|11a, –44.2/–43.9(?); 10s and 10a, unobs; 1b|8b, +18.4/+4.3. We do not know where to assign one of the +78.6 and +63.9 NMR splittings, making all assignments of the splittings under 2 G somewhat questionable.

C. 222/u322$^{\bullet+}$ (13). ESR (300 K): G 16.24 (2N). ENDOR (200 K): G 4.97 (vinyl), 4.24 (222 xi), 1.10, 0.77. Seven of the eleven different hydrogens are seen: δ +121.7 (assigned as 222 xo, 1.63 G), +96.9, +21.9, +13.4, –29.4, –53.7, –58.8. We presume that the two missing ones are at the [322] methylene on the node. Assignments based on analogy *222 ring:* 14x|15x, unobs; 4x|5x, +121.7; 14n|15n, –53.7; 4n|5n, –29.4; 3b|4b, +13.4/+21.9. *u322 ring:* 12v|13v, unobs; 9s|11s, +96.9; 9a|11a, –58.8; 10s and 10a, unobs; 1b|8b, +21.9/+13.4.

D. u222/322$^{\bullet+}$. NMR: Seven of the eleven different hydrogens are seen: δ +116.9, +43.5, +17.3, +0.8; –20.2, –40.7, –48.3. Assignments based on analogy *u222 ring:* 14v|15v, unobs; 4x|5x, +116.9; 4n|5n, –20.2; 3b|6b, +0.8/+17.3. *322 ring:* 12x|13x, unobs; 12n|13n, –40.7/–48.3; 9a|11a, –48.3/–40.7; 9s|11s, +43.5; 10s and 10a, unobs; 1b|8b, +17.3/+0.8.

Acknowledgment. This work was supported by the National Science Foundation (Grant CHE9105485), the National Institutes of Health (Grant GM 29549), and the Deutsche Forschungsgemeinshaft.